ce/papers Proceedings in civil engineering
eurosteel CRACOW 2026
WILEY

Full paper

A novel optimised additively manufactured connection for hybrid semi-rigid lightweight steel framing

Chuandong Xie[1] | Alireza Bagheri Sabbagh[1] | Ehsan Bakhshivand[1] | Ornella Iuorio[2]

Correspondence

Dr. Chuandong Xie
School of Engineering, University of Aberdeen, Aberdeen, UK, AB24 3FX
Email: chuandong.xie@abdn.ac.uk

[1] School of Engineering, University of Aberdeen, Aberdeen, UK, AB24 3FX
[2] Department of Architecture, Built Environment and Construction, Politecnico di Milano, Milan, Italy, 20133

Abstract

An innovative key-wheel (KW) connection comprising additive manufacturing (AM) wheel component is developed for a hybrid semi-rigid lightweight steel framing structure. The wheel components can be printed onto the web of the wall studs using either laser metal deposition (LMD) or wire arc additive manufacturing (WAAM). A genetic algorithm with multiple-objectives optimisation framework was employed to identify the optimal wheel geometries based on validated finite element method (FEM). For LMD connections, the objectives were to maximise the initial rotational stiffness, yielding strength and peak strength, while for WAAM connections an additional constraint was imposed by normalising these objectives with respect to material use. The optimisation results suggest a wheel shape with a greater number of elongated teeth for the proposed connection. The maximum joist deflections of the frame-level analysis are reduced by 16.5%-19.4% when employing the optimised connections, while the normalised initial stiffness, yield strength and peak strength are increased by 101.2%-103.9%, 166.7%-211.1% and 150.0%-158.3%, respectively.

Keywords

Lightweight steel framing, Metal additive manufacturing, Connection, LMD, WAAM, Optimisation

1 Introduction

Metal additive manufacturing (AM) has emerged as a transformative manufacturing technology, fundamentally shifting the production paradigm from material removal to material addition, in contrast to conventional manufacturing techniques [1, 2]. Substantial progress has been made in applying metal AM across a wide range of engineering disciplines, including aerospace [3], biomedical [4], mechanical [5], automotive [6] and shipbuilding [7] engineering. By integrating metal AM with conventional manufacturing (CM), a hybrid manufacturing approach has been developed [8, 9], enabling applications such as structural member strengthening [10, 11], connection enhancement [12, 13] and fatigue strengthening of damaged members [14, 15], among others.

To overcome the shear and pull-out failures at the corner screws and potentially premature failure issues at the joist-to-stud connections in lightweight steel framing (LSF) [16–19], a novel key-wheel (KW) connection has been developed [20] using two prevalent metal AM processes including laser metal deposition (LMD) and wire arc additive manufacturing (WAAM), as shown in Figure 1. This connection comprises a wheel-shaped component with multiple teeth printed onto the stud, together with a matching cut profile in the joist, enabling a semi-rigid moment-resisting connection. Seven parameters were defined to characterise the geometry of the wheel shape [20], as shown in Figure 2.

To determine the optimal wheel geometries for the proposed KW connection, a multi-objective optimisation framework based on a genetic algorithm was employed [21–24]. For connections manufactured using the LMD process, the optimisation aimed to maximise the initial rotational stiffness, yield strength and peak strength. For connections produced using the WAAM process, an additional constraint was introduced by normalising these objectives with respect to material use, in order to limit heat input and minimise distortion of the substrate. Structural-level analyses were subsequently conducted to compare the gravity-only and combined gravity and lateral loading responses of frames incorporating the original and optimised connections.

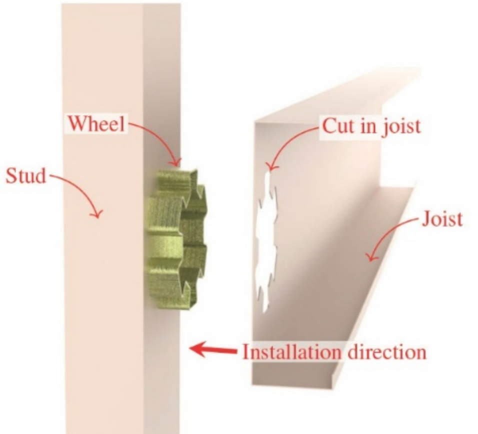

Figure 1 Key-wheel (KW) connection

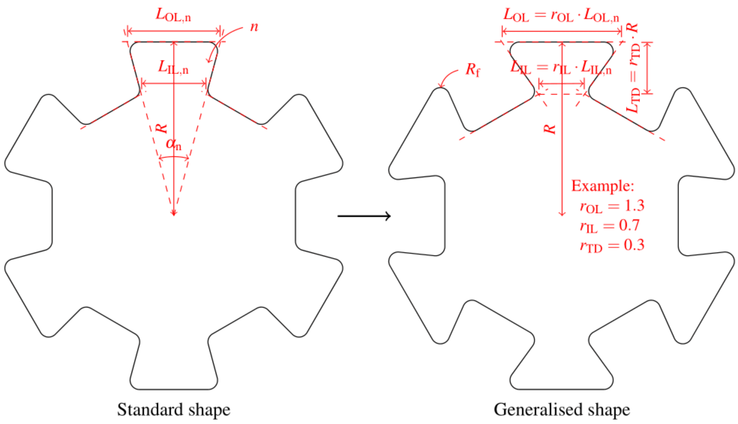

Figure 2 Wheel shape parameters

2 Optimisation framework

2.1 Objectives and design space

For the LMD process, the optimisation objectives were to maximise initial rotational stiffness k_e, yield strength M_y and peak strength M_u directly. For the WAAM process, these parameters were normalised by the volume of the wheel component of the wheel geometry to minimise heat input, represented by $\bar{k}_e$, $\bar{M}_y$ and $\bar{M}_u$, respectively. The initial rotational stiffness k_e, yield strength M_y and peak strength M_u were identified using an idealised moment-rotation relationship based on ASCE 41-23 [25], as shown in Figure 3.

Seven wheel-shape parameters including wheel radius R, tooth number n, outer length ratio r_{OL}, inner length ratio r_{IL}, tooth depth ratio r_{TD}, fillet radius of the corners R_f and wheel thickness t were investigated in the optimised procedure. The wheel radius R of 50 mm, 55 mm, 60 mm, 65 mm and tooth number n ranging from 3 to 12 with a step of 1 were considered. The outer length ratio r_{OL} and inner length ratio r_{IL} were both varied from 0.7 to 1.3 with a step of 0.01, and the tooth depth ratio r_{TD} ranged from 0.1 to 0.5 with a step of 0.01. The fillet radius R_f of 0.8 mm, 1.0 mm, 1.5 mm, 2.0 mm, 2.5 mm and 3.0 mm and wheel thickness t from 2.0 mm to 5.0 mm with a step of 0.5 mm were adopted.

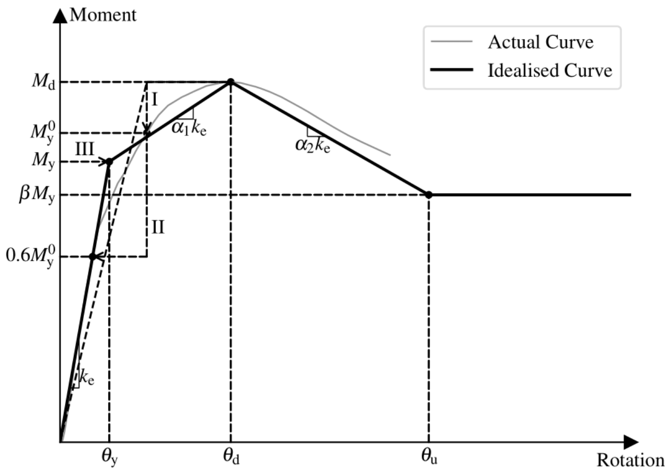

Figure 3 Idealised curve

2.2 Genetic algorithm implementation

A genetic algorithm (GA) was adopted for this multiple-objective optimisation procedure and implemented using the evolutionary computation framework Distributed Evolutionary Algorithms in Python (DEAP) [26]. To facilitate the modelling of wheel components, the open-source parametric three-dimensional modeler FreeCAD [27] was employed. The connection responses were obtained through the numerical analysis in Abaqus [28]. The objective values were subsequently extracted from the idealised moment-rotation curves. The overall optimisation process was executed in Python [29], interfacing with both FreeCAD and Abaqus. The population size and number of generations were both set to 150 to ensure a comprehensive exploration of the design space. Pareto-front selection was performed using the NSGA-III algorithm [30], where the Pareto front represents a set of mutually non-dominated solutions that capture trade-offs among the multiple objectives. The analysis steps as explained below.

Step 1: The initial generation was randomly created based on the prescribed parameter space.
Step 2: FreeCAD was used to generate IGES files describing the wheel geometry for each individual.
Step 3: Abaqus models were generated from the IGES files and submitted for finite element (FE) analysis.
Step 4: The fitness of each individual was evaluated based on the optimisation objectives derived from the idealised moment-rotation relationship.
Step 5: Pareto-based selection was performed using the NSGA-III algorithm.
Step 6: Crossover was applied to the selected individuals with an independent probability of 0.5.
Step 7: Mutation was applied to the offspring with an independent probability of 0.2.
Step 8: The termination criterion of 150 generations was checked. If not satisfied, the procedure returned to Step 2 using the updated population.

2.3 Finite element method and validation

The FE modelling of the connection is shown in Figure 4. Cold-formed steel (CFS) channel sections of 150M14-75 and 240M13-75, both with 15 mm lips were used for studs and joists, respectively. In the section labels, the leading number denotes the section depth in millimetres, followed by the thickness in tenths of a millimetre after the letter

"M", and ending with the flange width in millimetres. S450 steel, as specified in [31], was adopted for both the stud and joist, and its full stress–strain behaviour was modelled using the formulation proposed in [32]. For the wheel components manufactured using the LMD process, the constitutive model developed in [33] was adopted and calibrated against tensile coupon tests reported in [34]. The WAAM wheel components were modelled using the normal-strength steel constitutive model proposed in [35].

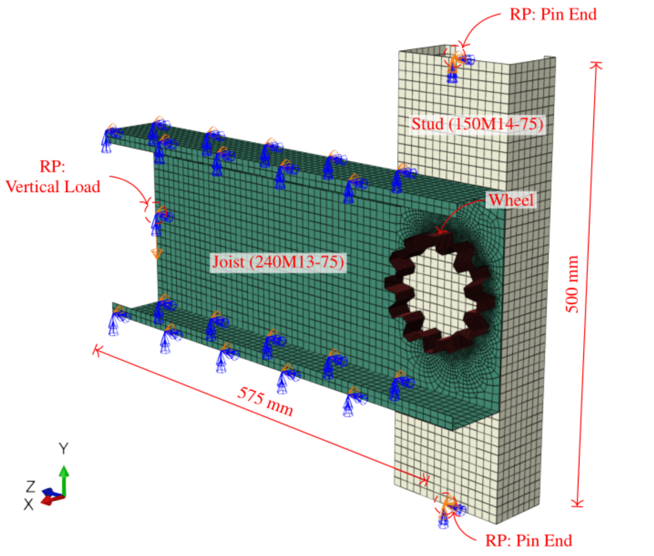

Figure 4 FE modelling of connection

All structural components were modelled using S4R shell elements. A global mesh size of 10 mm was applied to all CFS members, except at the joist ends, where a refined mesh size of 1 mm was employed. As the optimisation objectives were normalised, small clearance between the wheel and the joist cut was reasonably assumed to have a negligible influence on the optimisation outcomes. This gap was therefore neglected to accelerate the optimisation process and reduce computational cost. Contact interactions between all components, including joist-to-stud and joist-to-wheel, were defined using the *CONTACT PAIR algorithm with finite sliding in Abaqus. Tangential contact behaviour was modelled using a penalty formulation with a friction coefficient of 0.2 and a contact stiffness of 5.8 kN/mm. Normal contact behaviour was defined as "hard" contact with a nonlinear penalty formulation. Enhanced translational restraint in the global x-direction was applied to the joist to isolate the joist–wheel interaction. Geometric imperfections were introduced to provide a first-order representation of distortion caused by residual stresses and manufacturing deviations at the structural level [36]. A displacement-controlled vertical load was applied at the joist end, with a target corresponding to either a minimum of 80% post-peak strength degradation or a rotational drift of 0.04 rad, whichever occurred first. All moment responses were normalised by the bending capacity of the joist section.

The FE method was validated against cyclic tests of the KW-WAAM connection conducted by the authors. The R (measured from the geometric centre to the outer edge) was 55.8 mm, with a n of 4, r_{IL} and r_{OL} of 1.0, a r_{TD} of 0.3, a R_f of 3.0 mm, a wheel depth of 30.0 mm and a t of 3.3 mm. Based on the coupon test results, the thermal input only increases the yield and ultimate strengths by approximately 1.2%. Therefore, adopting the original CFS material properties, with slightly lower yield strength, is considered appropriate. Figure 5 shows the von-Mises stress distributions and the corresponding hysteretic curves. High stress concentrations and yielding were observed in the joist web surrounding the printed wheel, while the wheel itself remained elastic, consistent with the test observation. The proposed FE approach is capable of capturing the cyclic response of the KW-WAAM connection with reasonable accuracy in terms of overall behaviour, initial rotational stiffness and peak moment capacity.

3 Optimisation results

3.1 Pareto fronts

Figure 6 shows the Pareto fronts obtained for the KW-LMD and KW-WAAM connections after 150 generations. The parameter space is notably clear, yielding 46 and 24 optimised individuals, respectively. The optimisation suggests a wheel radius R of 65.0 mm, tooth number n of 12 and outer length ratio r_{OL} of 0.7 for KW-LMD connections. The inner length ratio r_{IL} and the tooth depth ratio r_{TD} are recommended within the ranges of 0.71-1.16 and 0.26-0.49, respectively, yielding a 12-elongated-rectangle-teeth profile. The fillet radius R_f is generally constrained between 0.8 mm and 1.5 mm, indicating a preference of sharper corners, with smaller fillet radii associated with higher initial rotational stiffness. The wheel thickness t varies from 2.0 to 4.0 mm, covering most practical design options, where individual thickness values preferentially enhance either the initial rotational stiffness or the yield and peak strengths. A clear trade-off is observed between the initial rotational stiffness and yielding strength, whereas the yield and peak strengths exhibit a positive correlation.

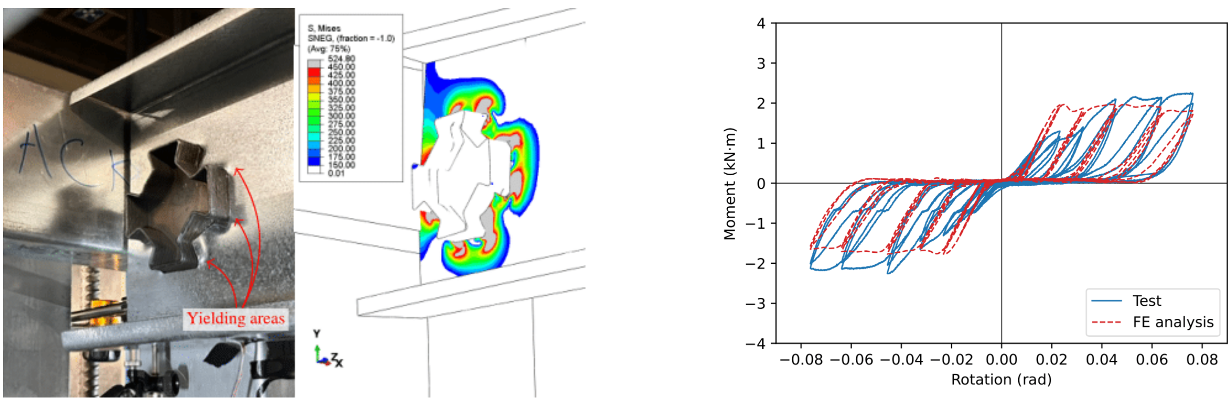

(a) Failure mode (b) Hysteretic curves

Figure 5 FE validation

For the KW-WAAM connection, all optimised individuals similarly adopt a wheel radius R of 65.0 mm, a tooth number n of 12, and a relatively small outer length ratio r_{OL} of approximately 0.7. However, the inner length ratio r_{IL} and tooth depth ratio r_{TD} are confined to narrower ranges of 0.89-1.29 and 0.20-0.28, respectively, indicating rectangular teeth that are shorter than those of the KW-LMD connections. The fillet radius R_{f} ranges from 1.0 mm to 2.0 mm, with smaller values again corresponding to higher initial rotational stiffness. Owing to the material use constraint, all KW-WAAM solutions adopt the minimum wheel thickness of 2.0 mm. The trade-off between initial rotational stiffness and yield strength remains evident, while no clear relationship is observed between the yield and peak strengths.

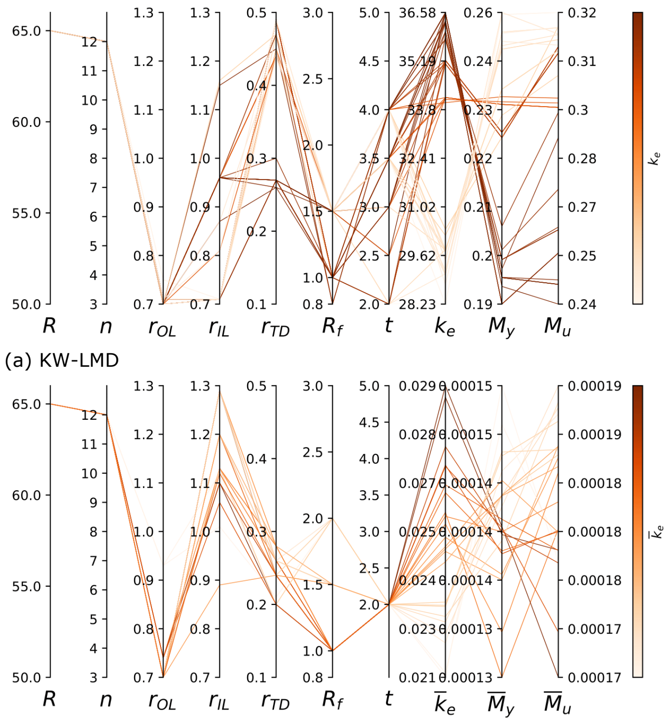

Figure 6 Pareto fronts

3.2 Optimised shapes

Table 1 summarises the optimised parameter ranges and presents two representative designs. The first corresponds to the individual with the highest initial rotational stiffness, while the second represents the optimal compromise solution selected using a weighted objective ratio of 0.4:0.4:0.2 for the (normalised) initial rotational stiffness, yield strength and peak strength, respectively. This weighting scheme accounts for all three objectives while maintaining a balanced performance in both the elastic and inelastic response stages. Across all optimised solutions, a wheel radius R of 65.0 mm is consistently recommended, regardless of the metal AM process employed. A tooth number n of 12 is also preferred to enhance the interlocking mechanism. In general, KW connections favour smaller outer and inner length ratios, resulting in narrow and elongated teeth, together with relatively small fillet radii. While a range of wheel thickness is viable for LMD-based connections, WAAM-based connections consistently adopt the minimum thickness of 2.0 mm to limit material use.

Table 1 Optimised results

LMD	WAAM
R = 65.0mm; n = 12; r_{OL} = 0.70-0.75; r_{IL} = 0.71-1.16; r_{TD} = 0.26-0.49; R_{f} = 0.8-1.5mm; t =2.0-4.0mm	R = 65.0mm; n = 12; r_{OL} = 0.70-0.93; r_{IL} = 0.89-1.29; r_{TD} = 0.20-0.28; R_{f} = 1.0-2.0mm; t =2.0mm
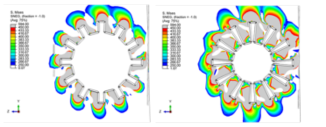	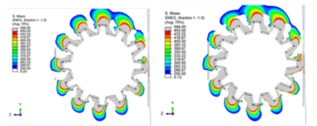

4 Frame level assessment

4.1 Model definition

To evaluate the frame-level performance, a H-frame configuration was modelled, incorporating conventional 3×3 screw connection with 5.4-mm-in-diameter screws, original (R = 65.0 mm, n = 4, r_{OL} = 1.0, r_{IL} = 1.0, r_{TD} = 0.3, R_{f} = 3.0 mm, t = 2.0 mm) and optimised KW-LMD (R = 65.0 mm, n = 12, r_{OL} = 0.70, r_{IL} = 0.71, r_{TD} = 0.49, R_{f} =1.0 mm, t = 3.5 mm) and KW-WAAM (KW-WAAM R = 65.0 mm, n = 12, r_{OL} = 0.70, r_{IL} = 1.29, r_{TD} = 0.24, R_{f} = 1.0 mm, t = 2.0 mm) connections. The original model employed a standard wheel shape, and the optimised shapes were taken from the second examples in Table 1, based on the weighted objective (0.4:0.4:0.2) for the (normalised) initial stiffness, yield strength and peak strength.

The FE modelling setup is shown in Figure 7. The frame configuration was derived from a six-storey building with a centre-to-centre span of 6000 mm and a storey height of 3000 mm. Each side frame was repeated at a spacing of 600 mm. CFS sections 150M14-75 and 142M12-70 were used for the studs and face tracks, respectively. Two CSF joist sections including 240M13-75 and 240M16-75 were considered to evaluate the improvements in mechanical performance provided by the optimised connections. Dead and live loads of 1 kN/m^2 and 2 kN/m^2, respectively, were applied to all floors in accordance with EN 1991-1-1 [37]. Pin-ended boundary conditions were assigned to the reference points coupling the tops and bottoms of the studs. Lateral translational restraints were also applied along the top edges of the joists to simulate the restraint provided by the floor sheathing.

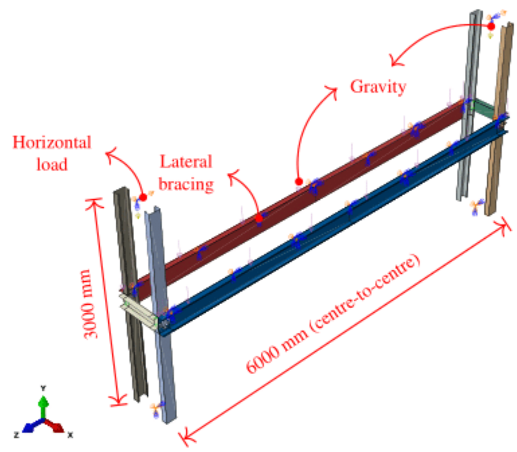

Figure 7 FE modelling of H frame

Two load cases were considered, including sole gravity loading and gravity loading combined with lateral pushover. The lateral pushover analysis targeted a drift corresponding to the lesser of 80% post-peak strength degradation or 4.0%, on the basis of the ultimate limit state. Gravity loads from the upper storeys were applied as concentrated loads at the reference points located at the tops of the studs, while gravity loads from the floor sheathing were applied as uniformly distributed loads on the top flanges of the joists. A storey weight of 10.66 kN was calculated in accordance with EN 1998-1-1 [38] and used to normalise the base shear.

4.2 Results

Figure 8 shows joist deflections and shear-drift curves obtained from the H-frame analyses. The H-frame with the original KW connection and 240M13-75 joists exhibited a 22.2% increase in joist deflection, together with reductions in initial rotational stiffness, yield strength and peak strength of 106.0%, 222.2% and 183.3%, respectively, compared with the H-frame incorporating conventional screw connections. By adopting the optimised KW connections, the joist deflection of the H-frame with KW-LMD connection was reduced by 19.4%, while the initial rotational stiffness, yield strength and peak strength increased by 102.2%, 211.1% and 158.3%, respectively. For the H-frame with KW-WAAM connections, the joists deflection was reduced by 16.5%, and the corresponding increases in initial rotational stiffness, yield strength and peak strength were 103.9%, 166.7% and 150.0%, respectively.

The enhanced mechanical performance of the optimised connections results in increased loading demands on the joists. When the joist section was upgraded from 240M13-75 to 240M16-75, the joist deflection of H-frames with KW connections was reduced by up to 21.8% compared with those using conventional connections. In addition, the initial rotational stiffness, yield strength and peak strength increased by 25.1%, 57.1% and 71.0%, respectively. Compared with conventional LSF systems, the AM-LSF system developed in this study offer enhanced design and manufacturing flexibility, faster construction, improved quality through reduced manual operations, and greater ease of dismantling and non-destructive deconstruction, thereby facilitating future adaption and reuse.

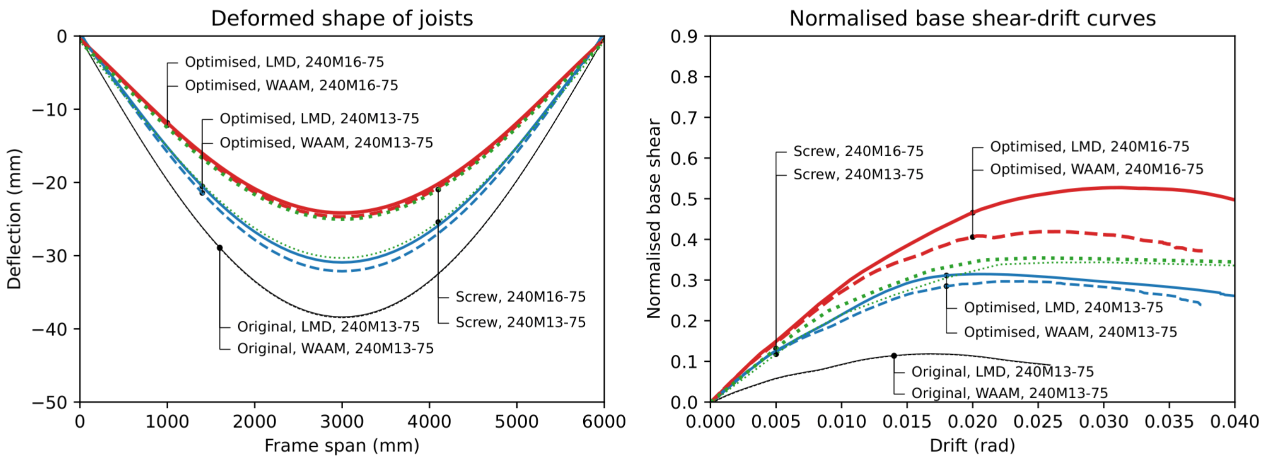

Figure 8 H-frame assessment

5 Conclusions

A multi-objective genetic algorithm optimisation framework was employed to identify optimal wheel geometries for additively manufacturing (AM) key-wheel (KW) connections in lightweight steel framing structures. Two metal additive manufacturing processes were considered, including laser metal deposition (LMD) and wire arc additive manufacturing (WAAM). The key findings and conclusions are summarised as follows:

(1) The optimisation results recommend a wheel geometry with 12 elongated teeth for the KW-LMD and KW-WAAM connections, with tooth depth ratios r_{TD} ranging from 0.26 to 0.49 and from 0.20 to 0.28, respectively.

(2) Trade-off behaviour was observed in both KW-LMD and KW-WAAM connections. Connections achieving higher (normalised) initial rotational stiffness tend to exhibit lower yield and peak strength values, and vice versa.

(3) Frame-level ultimate limit state analyses demonstrate that the implementation of optimised KW connections leads to substantial performance improvements compared with original KW connections. The maximum joist deflections are reduced by 16.5%-19.4%, while the normalised initial stiffness, yield strength and peak strength of the frames are increased by 101.2%-103.9%, 166.7%-211.1% and 150.0%-158.3%, respectively.

References

[1] Buchanan, C.; Gardner, L. (2019) *Metal 3D printing in construction: A review of methods, research, applications, opportunities and challenges*. Engineering Structures 180, p. 332–348.

[2] Raspall, F.; Araya, S.; Pazols, M.; et al. (2025) *Wire Arc Additive Manufacturing for Widespread Architectural Application: A Review Informed by Large-Scale Prototypes*. Buildings 15, H. 6, p. 906.

[3] Pant, H.; Arora, A.; Gopakumar, G.S.; et al. (2023) *Applications of wire arc additive manufacturing (WAAM) for aerospace component manufacturing*. The International Journal of Advanced Manufacturing

Technology 127, H. 11, p. 4995–5011.

[4] Ni, J.; Ling, H.; Zhang, S.; et al. (2019) *Three-dimensional printing of metals for biomedical applications*. Materials Today Bio 3, p. 100024.

[5] Gasser, A.; Backes, G.; Kelbassa, I.; et al. (2010) *Laser Additive Manufacturing: Laser Metal Deposition (LMD) and Selective Laser Melting (SLM) in Turbo-Engine Applications*. Laser Technik Journal 7, H. 2, p. 58–63.

[6] Alami, A.H.; Ghani Olabi, A.; Alashkar, A.; et al. (2023) *Additive manufacturing in the aerospace and automotive industries: Recent trends and role in achieving sustainable development goals*. Ain Shams Engineering Journal 14, H. 11, p. 102516.

[7] Taşdemir, A.; Nohut, S. (2021) *An overview of wire arc additive manufacturing (WAAM) in shipbuilding industry*. Ships and Offshore Structures 16, H. 7, p. 797–814.

[8] Baqershahi, M.H.; Ayas, C.; Ghafoori, E. (2024) *Design optimisation for hybrid metal additive manufacturing for sustainable construction*. Engineering Structures 301, p. 117355.

[9] Meng, X.; Gardner, L. (2025) *Hybrid construction featuring wire arc additive manufacturing: review, concepts, challenges and opportunities*. Engineering Structures 326, p. 119337.

[10] Gardner, L.; Li, J.; Meng, X.; et al. (2024) *I-section steel columns strengthened by wire arc additive manufacturing - concept and experiments*. Engineering Structures 306, p. 117763.

[11] Yang, J.; Wadee, M.A.; Gardner, L. (2025) *Strengthening of steel I-section beams by wire arc additive manufacturing — Concept and experiments*. Engineering Structures 322, p. 119113.

[12] Kanyilmaz, A.; Berto, F.; Paoletti, I.; et al. (2021) *Nature-inspired optimization of tubular joints for metal 3D printing*. Structural and Multidisciplinary Optimization 63, H. 2, p. 767–787.

[13] Laghi, V.; Babovic, N.; Benvenuti, E.; et al. (2024) *Blended structural optimization of steel joints for Wire-and-Arc Additive Manufacturing*. Engineering Structures 300, p. 117141.

[14] Ghafoori, E.; Dahaghin, H.; Diao, C.; et al. (2023) *Fatigue strengthening of damaged steel members using wire arc additive manufacturing*. Engineering Structures 284, p. 115911.

[15] Dahaghin, H.; Motavalli, M.; Moshayedi, H.; et al. (2024) *Wire and arc additive manufacturing for strengthening of metallic components*. Thin-Walled Structures 203, p. 112074.

[16] Bagheri Sabbagh, A.; Torabian, S. (2021) *Semi-rigid floor-to-wall connections using side-framed lightweight steel structures: Concept development*. Thin-Walled Structures 160, p. 107345.

[17] Ayhan, D.; Schafer, B.W. (2019) *Cold-formed steel ledger-framed construction floor-to-wall connection behavior and strength*. Journal of Constructional Steel Research 156, p. 215–226.

[18] Dai, Y.; Roy, K.; Fang, Z.; et al. (2023) *A critical review of cold-formed built-up members: Developments, challenges, and future directions*. Journal of Building Engineering 76, p. 107255.

[19] Jafarifar, N.; Bagheri Sabbagh, A.; Uchehara, I. (2023) *Rubberised concrete confined with thin-walled steel profiles; a ductile composite for building structures*. Structures 49, p. 983–994.

[20] Xie, C.; Bagheri Sabbagh, A.; Bakhshivand, E.; et al. (2026) *Shape optimisation of metal additive manufacturing connections in lightweight steel structures*. Journal of Constructional Steel Research 241, p. 110290.

[21] McCall, J. (2005) *Genetic algorithms for modelling and optimisation*. Journal of Computational and Applied Mathematics 184, H. 1, p. 205–222.

[22] Sivanandam, S.N.; Deepa, S.N. (2008) *Introduction to Genetic Algorithms*. Berlin, Heidelberg: Springer Berlin Heidelberg.

[23] Huang, D.; Pei, S.; Busch, A. (2021) *Optimizing displacement-based seismic design of mass timber rocking walls using genetic algorithm*. Engineering Structures 229, p. 111603.

[24] Hu, S.; Lei, X. (2023) *Machine learning and genetic algorithm-based framework for the life-cycle cost-based optimal design of self-centering building structures*. Journal of Building Engineering 78, p. 107671.

[25] ASCE (2023) *Seismic Evaluation and Retrofit of Existing Buildings (ASCE/SEI 41-23)*. Reston, Virginia: American Society of Civil Engineers.

[26] Fortin, F.-A.; De Rainville, F.-M.; Gardner, M.-A.; et al. (2012) *DEAP: Evolutionary Algorithms Made Easy*. Journal of Machine Learning Research 13, H. July, p. 2171–2175.

[27] FreeCAD Community (2025) *FreeCAD: Your own 3D parametric modeler*. .

[28] Dassault Systèmes Simulia Corp (2024) *Abaqus 2024*. .

[29] Python Software Foundation (2025) *The Python Language Reference* [online]. https://docs.python.org/3/reference/index.html [accessed on: 24 June 2025].

[30] Deb, K.; Jain, H. (2014) *An Evolutionary Many-Objective Optimization Algorithm Using Reference-Point-Based Nondominated Sorting Approach, Part I: Solving Problems With Box Constraints*. IEEE Transactions on Evolutionary Computation 18, H. 4, p. 577–601.

[31] Eurocode (2023) *Eurocode 3. Design of steel structures - General rules and rules for buildings (EN 1993-1-1)*. European Committee for Standardization.

[32] Gardner, L.; Yun, X. (2018) *Description of stress-strain curves for cold-formed steels*. Construction and Building Materials 189, p. 527–538.

[33] Hradil, P.; Talja, A.; Real, E.; et al. (2013) *Generalized multistage mechanical model for nonlinear metallic materials*. Thin-Walled Structures 63, p. 63–69.

[34] Cacace, S.; Furlan, V.; Sorci, R.; et al. (2020) *Using recycled material to produce gas-atomized metal powders for additive manufacturing processes*. Journal of Cleaner Production 268, p. 122218.

[35] Huang, C.; Kyvelou, P.; Gardner, L. (2023) *Stress-strain curves for wire arc additively manufactured steels*. Engineering Structures 279, p. 115628.

[36] Weber, B.; Meng, X.; Gardner, L. (2026) *Optimised and 3D printed steel garden bridge: from design to experimental verification*. Automation in Construction 181, p. 106638.

[37] Eurocode (2002) *Eurocode 1. Actions on structures - General actions - Densities, self-weight, imposed loads for buildings (EN 1991-1-1)*. European Committee for Standardization.

[38] Eurocode (2013) *Eurocode 8: Design of structures for earthquake resistance – Part 1: General rules, seismic actions and rules for buildings (EN1998-1-1)*. European Committee for Standardization.